

# Synthesis of Fibrous-Like Stripes ZnO: Ce Nano Structures for NO<sub>2</sub> and NH<sub>3</sub> Sensing

Raad S.Sabry<sup>1</sup>, Mohammed J.Hassan<sup>2</sup>, Tagrhid S. Muhsin<sup>1</sup>, Baker A. Joda<sup>3</sup>

Department of Physics, College of Sciences, University of Al-Mustansiriya University, Baghdad, Iraq<sup>1</sup>

Department of Chemistry, College of Sciences, University of Al-Mustansiriya, Baghdad, Iraq<sup>2</sup>

Department of Chemistry, College of Science, University of Kerbala, Karbala, Iraq<sup>3</sup>

**ABSTRACT:** Zinc oxide and Ce doped nanostructures thin films with different ZnO:Ce ratios (3, 5 and 10) wt% have been prepared by Sol-gel spin coating method at optimum annealing temperature of 550 °C. The synthesized samples were characterized by X-ray diffraction (XRD), the spectra of the pure and ZnO: Ce nanostructures correspond to the various planes of a hexagonal ZnO phase, also the crystalline size decreased from about 37nm to 27nm by increasing Ce concentration, atomic force microscopy (AFM) analysis shows that the surface roughness of the samples increased from 1.14 for pure ZnO to 2.15 nm for 10% doping. FESEM measurements show that the ZnO is spherical shape particles which transfers into fibrous-like stripes embedded within a wrinkled shape with different size depending upon the Ce concentration. This change in the surface shape can improve the NO<sub>2</sub> and NH<sub>3</sub> sensing in the two cases of gas sensing measurements, namely static and dynamic case. It was found that the sensitivity was increased by using the same operating temperature. The dynamic results show that the response and recovery times are improved when the Ce concentration is increased. The optical measurements are shown that the transmittance was decreased with increasing of Ce concentration in zinc oxide.

**KEYWORDS:** NO<sub>2</sub>, NH<sub>3</sub>; Fibrous-like stripes, FESEM, ZnO: Ce nanostructures.

## I. INTRODUCTION

Metal oxide semiconductors (MOSs) have been used as photo catalysts and other applications such as chemical sensors, detecting ultraviolet (UV) radiation, photoconductivity, gas sensory chemical sensors, and optoelectronic devices. Recently, ZnO has received the attention of many scientific researchers due to its remarkable combination of physical and optical properties. In addition, it has a wide band gap (3.37 eV at room temperature), high excitation binding energy (60 meV) [1, 2]. It was found that ZnO can use in various fields such as transparent electrode, gas sensors, room temperature ultraviolet lasers, solar cell windows, photovoltaic devices, catalysts, and piezoelectric cells [3–5]. Several deposition methods have been used to carry out undoped and doped ZnO films such as sputtering, pulsed laser deposition, vapor–liquid–solid (VLS) and hydrothermal, and sol–gel process [2,6]. The last method, namely sol–gel process has several advantages when compared with other methods due to its simplicity, easy control of the film deposition, safety as well as low cost of the apparatus and raw materials [7]. A doping is an effective way to improve the properties of ZnO thin films. Therefore, adding selective elements to ZnO offers an important route to enhance and control its optical and electrical properties, which are crucial to its practical applications [8–10]. In recent years, many of rare earth elements such as Sc, Y, Ce, Eu, and Er have been added to ZnO, but the use of cerium doping has received more attention due to its important properties including: (a) the redox couple Ce<sup>+3</sup>/Ce<sup>+4</sup> that makes cerium oxide shift between CeO<sub>2</sub> and Ce<sub>2</sub>O<sub>3</sub> under oxidizing and reducing conditions and (b) the easy formation of labile oxygen vacancies with the relatively high mobility of bulk oxygen species [11-13]. Therefore, the versatile properties of Ce-doped ZnO nanostructures have been explored for many applications such as photoluminescence, photo electro chemical properties under visible light, and as well as chemical and gas sensors [11]. The main aim of this study is to develop and validate the use of doping on structural and optical properties of the Ce (3,5 and 10 at.wt.%) - ZnO sol–gel deposited thin films by using various characterization of the target gas sensor.

# International Journal of Innovative Research in Science, Engineering and Technology

(An ISO 3297: 2007 Certified Organization)

Vol. 4, Issue 8, August 2015

## II. MATERIALS AND METHODS

In this study, zinc acetate dihydrate ( $\text{Zn}(\text{CH}_3\text{COO})_2 \cdot 2\text{H}_2\text{O}$ , BDH, 98.5%) and cerium nitrate hexahydrate ( $\text{Ce}(\text{NO}_3)_3 \cdot 6\text{H}_2\text{O}$ , BDH, 99%) were used as starting material and doping sources, respectively. Moreover, ethanol ( $\text{C}_2\text{H}_5\text{OH}$ , Fluka, 99.9%) and monoethanolamine (MEA) ( $\text{C}_2\text{H}_7\text{NO}$ , Fluka, 98 %) were used as a solvent and stabilizer, respectively. In the preparation procedure for ZnO: Ce thin films, Zinc acetate dihydrate was dissolved in a mixture which was composed of ethanol and MEA at  $70^\circ\text{C}$ . The molar ratio of MEA to zinc acetate dihydrate maintained at 1 and the concentration of zinc acetate was 0.75 mol/L. The mixed solution was stirred at  $70^\circ\text{C}$  for one hour, then ethanolic solution of cerium nitrate hexahydrate with optimized Zn/Ce ratio at (3,5 and 10)% was added to mixture. The final solution was stirred for an additional hour. After stirring, the solution becomes clear and homogeneous. This solution was used as the coating solution after cooling at room temperature then allowed to age for 24h before initiating deposition. The films were obtained by a spin-coating procedure. The aged solution was dropped on glass substrates, which were rotated at 500 rpm for 10 sec, after that the speed was increased to 2000 rpm for 30 sec and 3000 rpm for 30 sec. After the coating step, the films were dried at  $100^\circ\text{C}$  for 10 min. This step was repeated for ten times to obtain thickness about 325 nm, finally they were annealed at  $550^\circ\text{C}$  in air for 1 h at rate of 10 min.

## III. INSTRUMENTATION

The structure and lattice parameters of pure and ZnO:Ce films were analyzed by XRD instrument (MINIFLEX II RIGAKU, Japan), with the following specifications Cu ( $K\alpha$ ) radiation with  $\lambda = 1.5405 \text{ \AA}$  (40 kV, 30 mA). The morphological properties of all films were investigated and observed by field emission scanning electron microscope (HITACHI S-4160) made in Japan. The optical transmittance and absorption were measured with a range of (300-900 nm.) by using (UV-1650PC Shimadzu software 1700 1650, UV-Visible recording Spectrophotometer, Japan). The surface morphological of ZnO thin films were analyzed using atomic force microscopy (SPM,AA-3000USA).

## IV. RESULTS AND DISCUSSIONS

Figure.1 shows the typical XRD pattern of pure ZnO and ZnO:Ce thin film. The major peaks are identified as (1 0 0), (0 0 2), (1 0 1), (1 0 2), (1 1 0), and (1 0 3), plane of reflections for a single phase wurzite structure of ZnO and the peak located at  $2\theta = 28.7^\circ$  is attributed to (1 1 1) plane for the  $\text{CeO}_2$  cubic structure (JCPDS standard card No. 75-0390) crystalline structure. Therefore, the diffraction peaks of pure ZnO and ZnO:Ce, without characteristic peaks of other impurities, are indexed to the ZnO hexagonal wurzite structure according based on its JCPDS standard card (No. 75-0576). The average crystalline size (D) was also estimated by using scherrer's formula,  $D = 0.9\lambda/(\beta\cos\Theta)$ , based on the integral width of XRD peaks, where  $\lambda$  is the wavelength of the incident X-ray radiation,  $\beta$  is the full width at half-maximum (FWHM) of the desired peak (here (1 0 1) at  $2\theta = 36.3^\circ$ ) in radians and  $\Theta$  is the diffraction angle.

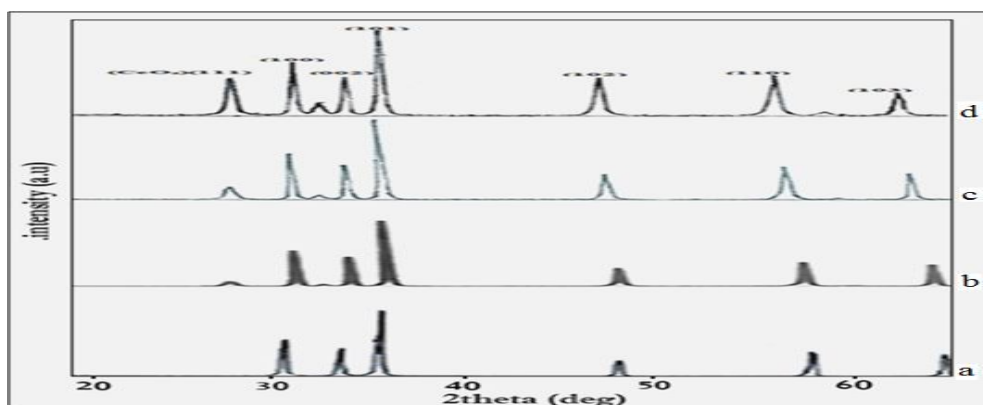


Figure 1: XRD patterns of ZnO thin film with different Ce concentrations: (a) pure (b) 3% Ce, (c) 5% Ce and (d) 10% Ce.

## International Journal of Innovative Research in Science, Engineering and Technology

(An ISO 3297: 2007 Certified Organization)

Vol. 4, Issue 8, August 2015

The crystalline structure and averaged crystal size for different Ce doped ZnO system was summarized in Table.1. It was found that when increasing cerium concentration in the films, the average crystalline size decreased.

Table 1: Crystalline properties of pure ZnO and ZnO:Ce thin films.

Samples	Average grain size/ nm
Pure	37.1
3 %	33.9
5 %	32.4
10 %	27.0

This can be explained because as ionic radii of  $Ce^{+3}$  are 0.092 nm which are larger than that of  $Zn^{+2}$  ion of 0.074 nm, therefore, it is difficult for  $Ce^{+3}$  to enter the crystalline lattice of ZnO to substitute  $Zn^{+2}$ . The  $Ce^{+3}$  ions seem more likely to form complex with the surface oxygen of ZnO, which decreases the growth of ZnO crystallite [14, 15].

The results in Figure 2(a) show that the nanoparticles and a smooth grains to be formed. Interestingly, similar results were also reported in the literature by other authors [16].

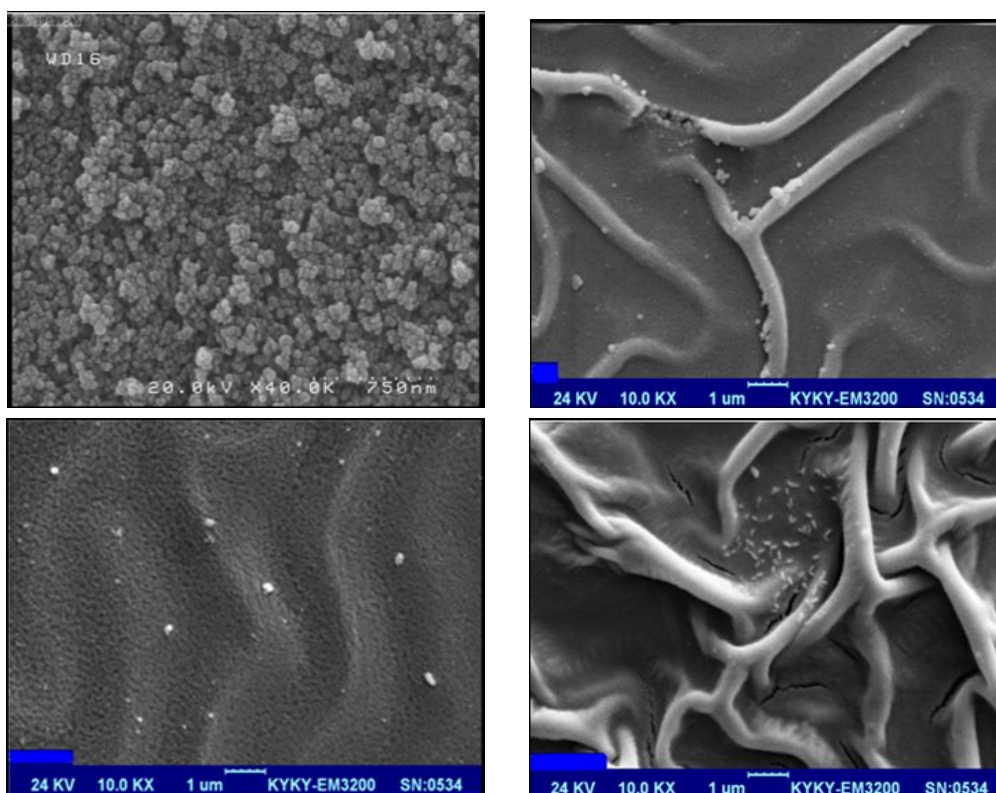


Figure 2: FE-SEM images of (a) pure ZnO (b) 3% Ce, (c) 5% Ce and (d) 10% Ce.

In general the film is homogeneous, continuous and uniform distribution and Spherical shape. An image of 3% Ce concentration shows that the films consist of small regions of fibrous-like stripes (ZnO:Ce) embedded within a wrinkled, as shown in Figure 2 (b). A previous study has suggested the two mechanisms can be used to explain wrinkle formation. The main reason may be related to the increase in volumetric strain [17]. Another reason is that a substantial loss of the hydroxyl/alkoxy groups during annealing induced stress formation [18]. Figure 2 - (c) shows that the SEM micrographs of a typical ZnO:Ce nanostructure hybrid the ZnO:5% Ce has a wrinkled/perturbed morphology with

## International Journal of Innovative Research in Science, Engineering and Technology

(An ISO 3297: 2007 Certified Organization)

Vol. 4, Issue 8, August 2015

small patches scattered on its surface. It was found that the increase of Ce (5%) lead to decrease the volume and height of ganglia-like, as shown in Figure 2(c). On the other hands, the results in Figure 2 (d) show that increase of Ce (10%) lead to increase the volume and height of the ganglia-like content and become more complex. Therefore, it looking more distorted and branched at their ends, induced pronounced wrinkling, Bulk shrink age is most likely caused by rapid solvent evaporation. The derived films evolve from desorption of the hydroxyl groups with subsequent ZnO: Ce crystallization. It was found that a wrinkle formation is beneficial and prestressing phase effectively reduces the intrinsic stress within the film during operation making the hybrid nanostructure.

Figure 3 (a,b,c,d) Shows the pure ZnO and ZnO:Ce thin films at different concentration (3, 5 and 10) % ,annealed in 550°C for 2h. The root mean square (RMS) surface roughness is observed to be 0.693, 1.14, 1.47 and 2.15 nm for a, b, c, and d samples, respectively when compared with the pure ZnO. The roughness is increased with increasing the cerium concentration in the films. This increase is attributed to the difference in ion size between Zn ( $r_{Zn^{2+}} = 0.074$  nm) and Ce ( $r_{Ce^{3+}} = 0.092$  nm).

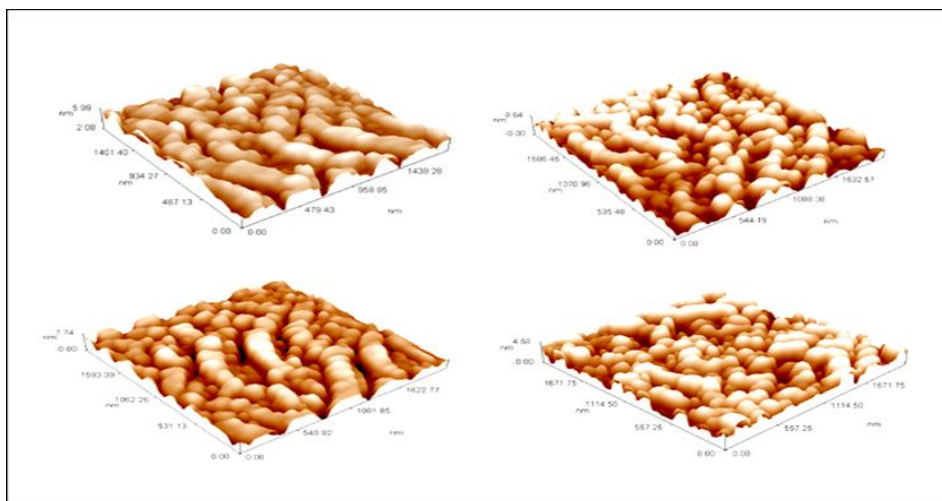


Figure 3: AFM three-dimensional images of ZnO surface with different concentrations of Ce.

Figure 4 shows the optical transmittance spectra for ZnO and ZnO doped Ce thin films using the UV–visible wavelength (350–800 nm).

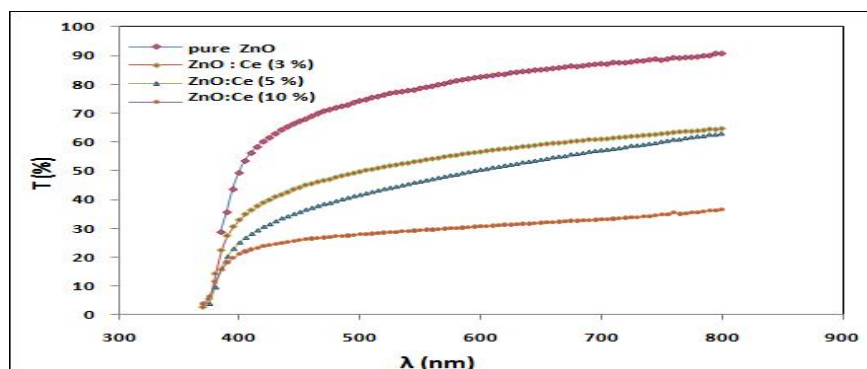


Figure 4: Transmittance spectra of ZnO thin film with different concentrations of Ce.

In the light of these results, it can be seen that the transmittance of pure ZnO thin films were measured at approximately 95% in the visible light ranged from 370 to 800 nm. It was found that, the percentage of transmittance is decreased

## International Journal of Innovative Research in Science, Engineering and Technology

(An ISO 3297: 2007 Certified Organization)

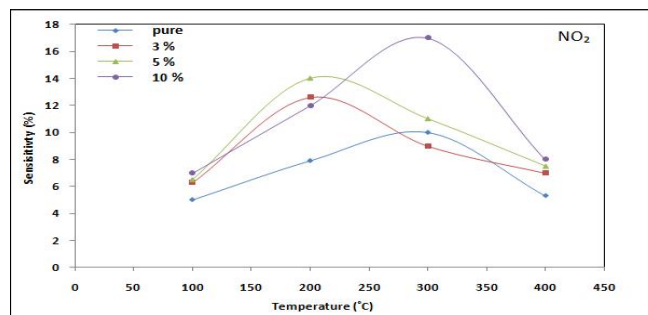
Vol. 4, Issue 8, August 2015

until 10% ZnO when the concentration values of ZnO:Ce thin film increase. This reduction in the transmittances of the ZnO doped Ce thin films may be due to the observed morphology for the corresponding sample. According to AFM analysis, there is a difference in the measured root mean square (rms) surface roughness values between samples. The rms values, namely 0.693, 1.14, 1.47, and 2.15 nm were determined for pure, 3, 5, and 10 % ZnO doped Ce samples, respectively. The findings show that the sample with the highest Ce doping Ce (10 %) has the largest surface roughness. As a result it has the highest scattering and the lowest transmittance. Moreover, the RMS surface roughness of the 3% ZnO doped Ce sample is lower than the 5 % ZnO doped sample. Thus, the higher measured transmittance is due to lower scattering of this sample. According to these results, the values of band gap energy for ZnO and 3, 5, and 10% of Ce were found to be 3.219, 3.222 and 3.232 eV, respectively.

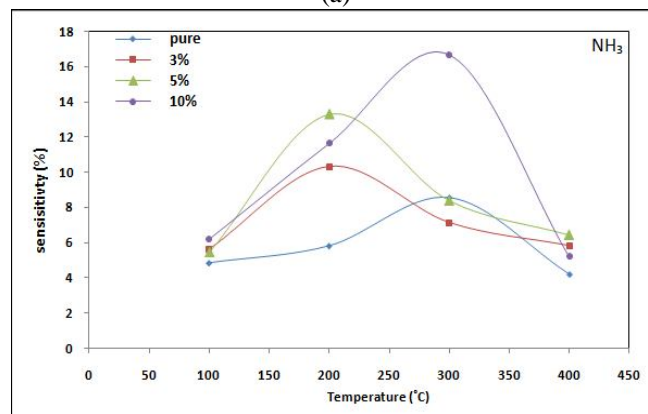
The gas sensing behavior of pure ZnO and ZnO: Ce thin films annealed at 550°C were studied by using static and dynamic measurements system. The thin films resistors were measured in air and 100 ppm of NH<sub>3</sub>, and NO<sub>2</sub> as well. The operating temperature was range at the interval of 100 to 400 °C. The sensitivity value of gas was determined at particular operating temperature by using the following equation.

$$S = \left| \frac{R_g - R_a}{R_a} \right| \times 100$$

Where  $R_a$  is electrical resistance of the sensor in air,  $R_g$  is electrical resistance of the sensor in gas. Figure 5 shows the variation of the sensitivity with temperature for pure and ZnO: Ce (3%, 5 %, and 10 %) sensor samples toward 100 ppm NH<sub>3</sub> and NO<sub>2</sub> gases.



(a)



(b)

Figure 5: Sensitivity of ZnO thin film with different Ce concentrations as a function of operating temperature for NO<sub>2</sub> (a) and NH<sub>3</sub> gases (b).

It can be seen that the sensitivity for all the samples gradually increases with increasing the temperature values to reach the maximum values, and then it is dropping at high temperature. The maximum values corresponding to an optimum operating temperature for NH<sub>3</sub> and NO<sub>2</sub> were appeared at 300°C for pure and 10 % samples and 200 °C for 3 % and 5 %

## International Journal of Innovative Research in Science, Engineering and Technology

(An ISO 3297: 2007 Certified Organization)

Vol. 4, Issue 8, August 2015

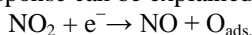
samples, as shown Table 2. The change in the sensitivity with temperature depends on the interaction between the adsorbed oxygen species and gases [19, 20]. When the pure and ZnO:Ce sensor samples are heated, the oxygen molecules begin to adsorb and dissociate ( $O_2 \rightarrow 2O^- \rightarrow O^{2-}$ ) on their surfaces and its concentration rise gradually with increasing the temperature until certain temperature which accompanied with the increase in the electrical resistance. While at higher temperatures, desorption of oxygen species from the sensor surfaces leads to decrease the concentration of oxygen species. So, the high sensitivity values of gases at temperature of 300°C can be to the high concentration of adsorbed oxygen species and high oxidation activity of gases [21-23]. The results in Table 2 show that the sensitivity is increased when the concentration of Ce increase. A possible explanation is that the addition of Ce may be caused to decrease the particle size, as shown from the XRD analysis. As a result, the change in the surface shape from smooth to Wrinkle is also found, as shown from FE-SEM measurements. This means that an increasing in the surface to volume ratio leads to enhance the interactions between the cases and surface. The results of AFM analysis show that the roughness is increased when the concentration of Ce increase, and lead to produce a largest effective surface area in order to react with the gas.

Table 2: Sensitivity of ZnO and ZnO:Ce using the operating temperatures ranged from 200 to 300 °C for NO<sub>2</sub> and NH<sub>3</sub> gases.

Doping	Sensitivity%			
	NO <sub>2</sub>		NH <sub>3</sub>	
	200°C	300°C	200°C	300°C
Pure ZnO	5.80	8.54	7.9	10
3%	10.31	7.12	12.6	9
5%	13.28	8.83	14.0	11
10 %	11.64	16.66	12.0	17

Figure 6 show the measured resistances against the values of time for pure, 3, 5, and 10 % ZnO doped Ce samples by using various concentrations of gases, namely 100, 150, and 200 ppm of NH<sub>3</sub> and NO<sub>3</sub> at room temperature. It can be seen that the resistance increased with increasing the concentrations of gases during the exposure to gases (NO<sub>2</sub> and NH<sub>3</sub>). In addition, the minimum resistances are observed at concentration of 10% Ce for two gases, whereas the maximum values observed at 3% concentration of Ce and pure ZnO for NH<sub>3</sub> and NO<sub>2</sub> gas, respectively.

The response and recovery times for sensor were reduced for all samples when the concentrations of Ce increase, as shown in Table 3. Moreover, the minimum response and recovery times are observed at the concentration of 10% Ce. It was found that the values of resistance are increased for NH<sub>3</sub> exposure when compared to NO<sub>2</sub>, as shown in Figure 6. A relative change in the electrical conductance due to an oxygen ion acts as a trap to electrons from the thin films. The electrons are taken from ionized donors through conduction band. The density of majority charge carriers at the gas–solid interface was reduced. This leads to form a potential barrier for electrons with increasing the density of oxygen ions on the surface. The adsorption of further oxygen is inhibited. Thus at the junctions between ZnO grains, the depletion layer and potential barrier leads to the increasing of the electrical resistivity value. This value is strongly dependent on the concentration of adsorbed oxygen ions on the surface. Introducing the n-ZnO films in an NH<sub>3</sub> ambient will change the concentration of these ions and increase the resistance. These results are in agreement with those reported in the literatures [23-25]. The detection of an oxidizing gas such as NO<sub>2</sub> can be associated with reaction in which conduction electrons are consumed and the subsequent detection reaction lead to increase the barrier height and increase the surface resistance. The NO<sub>2</sub> response can be explained below:



The electrons consumed in these reactions are extracted from the conduction band, thus raising the resistivity of Ce-doped zinc oxide film. It is necessary to mention that in the last case, the reaction products emerging from the primary detection reactions escape further detection within the sensing layer. The improvement of sensing properties of doped zinc oxide sensor structure towards hazardous gas is determined by the use of a particular dopant for the detection of specific gas species. The presence of chemical adsorbed molecules (NO<sub>2</sub>) may be caused electron depletion in the thin

## International Journal of Innovative Research in Science, Engineering and Technology

(An ISO 3297: 2007 Certified Organization)

Vol. 4, Issue 8, August 2015

film surface and the building up of a Schottky surface barrier; consequently, the electrical resistivity of the thin film increases to a maximum value [26, 27].

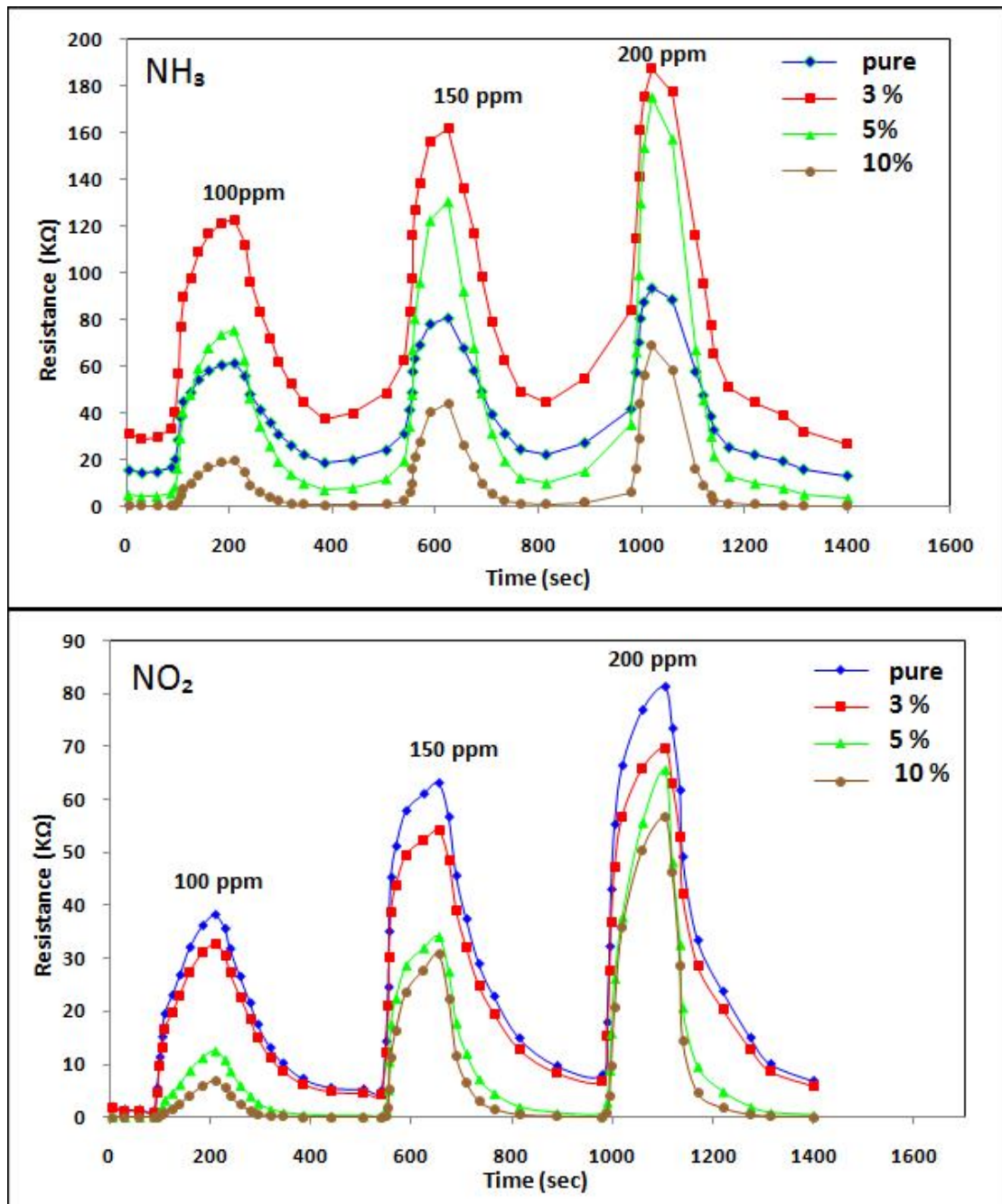


Figure 6: Dynamic response of the conduct metric sensor to various concentrations of  $\text{NO}_2$  and  $\text{NH}_3$  gases at Room temperature.

# International Journal of Innovative Research in Science, Engineering and Technology

(An ISO 3297: 2007 Certified Organization)

Vol. 4, Issue 8, August 2015

Table 3: Response and Recovery time values of ZnO and various ZnO:Ce.

Sample	Response time (s)			Recovery time (s)		
	100ppm	150 ppm	200ppm	100 ppm	150 ppm	200 ppm
NH <sub>3</sub> gas						
pure	85	97	130	112	115	190
3 % Ce	120	122	125	130	135	155
5 % Ce	80	99	121	110	119	135
10 % Ce	70	90	115	105	111	120
Sample	Response time (s)			Recovery time (s)		
NO <sub>2</sub> gas						
pure	121.1133	105.566	120.352	130.759	135.68	200.5
3 % Ce	98.9263	114.566	124.383	120.206	140.393	150.22
5 % Ce	94.255	110.566	111.837	115.293	120.293	117.3
10 % Ce	65.1063	78.343	85.29	93.92	95.56	98.47

## V. CONCLUSION

In conclusion, the results of FE-SEM are shown that the structures for pure ZnO thin films are spherical, nanoparticles distributed a regular, basis and homogeneous, while doped thin films were shapes like fiber and a wrinkle network. On the other hands, the findings of AFM technique are indicated that the roughness increased with increasing the cerium concentration in the films from (1.14) to (2.15). The optical properties of undoped and Ce doped ZnO films were shown that the higher transmittance (95%) was found for undoped ZnO films when compared with (65-40%) for doped Ce films within wavelength ranged (350-900nm). The energy gap is slowly increased when the doping increase. The energy gap is slowly increased when the doping increase. Furthermore, the sensitivity of all the samples is increased when the operating temperature increase. It was found that the maximum value was reported corresponding to an optimum operating temperature, which is 300°C for sample (10 %) and 200 °C for samples (3 % ,5 % ). The results of dynamic sensitivity at room temperature have concluded that the 3% doping have a maximum resistance for NH<sub>3</sub> while pure ZnO have a maximum value for NO<sub>2</sub> gas.

## REFERENCES

- [1] M. Dutta, S. Mridha, D. Basak, " Structural, Optical, and Electrical Properties of ZnO Thin Films Prepared by Spray Pyrolysis: Effect of Precursor Concentration" Appl. Surf. Sci, No. 254, pp. 2743, 2008.
- [2] R.S. Sabry, O. AbdulAzeez, "Hydrothermal growth of ZnO nano rods without Catalysts in a single step "Manufacturing Letters elsevier, Vol. 2, pp. 69–73, 2014.
- [3] O. Lupan , Lee Chow , G. Chai,," A single ZnO tetrapod-based sensor " Sensors and Actuators B: Chemical, Vol. 141 ,pp. 511–517 2009.
- [4] K.-S. Ahn, Y. Yan, S. Shet, T. Deutsch, J. Turner, M. Al-Jassim, " Enhanced Photo electrochemical Responses of ZnO Films Through Ga and N Co doping" Appl. Phys. Lett, Vol.91, No.23, pp.1909, 2007 .
- [5] Z. Lin Wang and J. Song, " Piezoelectric Nanogenerators Based on Zinc Oxide Nanowire Arrays", SCIENCE " ,Vol. 312 ,No. 23, pp. 242-246 2006.
- [6] S. Ma, R. Li , C. Lva, W. Xu, X. Gou, " Facile synthesis of ZnO nanorod arrays and hierarchical nanostructures for photocatalysis and gas sensor applications", Journal of Hazardous Materials, Vol. 192 , pp. 730– 740, 2011.
- [7] A. Abdel Aal ,Sawsan A. Mahmoud, A. Aboul-Gheit" Sol–Gel and Thermally Evaporated Nanostructured Thin ZnO Films for Photocatalytic Degradation of Trichlorophenol", Nanoscale Res Lett, Vol. 627–634 ,pp.93,2009 .
- [8] P. Partha. Pal, J. Manam, " EFFECT OF Li+ CO-DOPING ON THE LUMINESCENCE PROPERTIES OF ZnO: Tb3+ NANOPHOSPHORS", NANOSYSTEMS: PHYSICS, CHEMISTRY, MATHEMATICS No.3 ,Vol.4 ,pp 395–404 , 2013 .



## International Journal of Innovative Research in Science, Engineering and Technology

(An ISO 3297: 2007 Certified Organization)

Vol. 4, Issue 8, August 2015

- [9] Ch. Ge, Ch. Xie, Sh. Cai, "Preparation and gas-sensing properties of Ce-doped ZnO thin-film sensors by dip-coating" Mater. Sci. Eng., No. 3 B, Vol.137, pp. 53-58 2007.
- [10] M.F. Al-Kuhaili, S.M.A. Durrani, I.A. Bakhtiari, "Carbon monoxide gas-sensing properties of CeO<sub>2</sub>-ZnO thin films", Appl. Surf.Sci, Vol. 255, pp. 3033-3039 2008 .
- [11] G.N. Dar, Ahmad Umar, S.A. Zaidi, Ahmed A. Ibrahim, M. Abaker, S. Baskoutas, M.S. Al-Assiri, " Ce-doped ZnO nanorods for the detection of hazardous chemical" Sensors and Actuators B , Vol. 173 , PP. 72– 78 2012 .
- [12] K.R.Nemade, S.A.Waghuley, Gas Sensing Parameters: Resolution Limit and Hysteresis of ZnO and CeO<sub>2</sub> MOXs Films", Global Journal of Science, Engineering and Technology ISSN: 2322-2441 , Issue 2, 201, 7-12.
- [13] Ch. Liu, X. Tang, C. Mo, Zh. Qiang," Characterization and activity of visible-light-driven TiO<sub>2</sub> photocatalyst co doped with nitrogen and cerium", J. Solid State Chem, Vol. 181 ,No.4, pp. 913-919 2008.
- [14] M. Yousefi, M. Amiri, R. Azimirad, A.Z. Moshfegh, "Enhanced photoelectrochemical activity of Ce doped ZnO nanocomposite thin films under visible light", Journal of Electroanalytical Chemistry, No.661, pp. 106–112, 2011.
- [15] Yong-Il Jung, Bum-Young Noh, Young-Seok Lee, Seong-HoBaek, Jae Hyun Kim and Il-Kyu Park," Visible emission from Ce-doped ZnO nanorods grown by hydrothermal method without a post thermal annealing process", Nanoscale Research Letters , 7:43, Vol. 7, pp. 43, 2012.
- [16] N. Nagarani, Department of Physics SMGCW and V. Vasu, "Structural and Optical Characterization of ZnO thin films by Sol- Gel Method", Journal on Photonics and Spintronics, Vol.2, No.2, 2013.
- [17] S.J. Kwon, J.H. Park, J.G. Park , "Wrinkling of a sol-gel-derived thin film", Physical Review E vol.71, p.11604 2005.
- [18] G.W. Scherer, "Sintering of sol-gel films", Journal of Sol-Gel Science and Technology, vol.8 , p.353–363, 1997
- [19] S. D. Shinde, G. E. Patil, D. D. Kajale, D. V. Ahire, V. B. Gaikwad and G. H. Jain, "Synthesis of ZnO nanorods by hydrothermal method for gas sensing applications", International Journal on Smart Sensing and Intelligent Systems, Vol. 5, No. 1, pp. 57-70, 2012.
- [20] L. Wang, Y. Kang, X. Liu, S. Zhang, W. Huang and S. Wang, "ZnO nanorod gas sensor for ethanol detection", Sensors and Actuators B, Vol. 162, pp. 237- 243, 2012.
- [21] C. Ge, C. Xie, M. Hu, Y. Gui, Z. Bai and D. Zeng, "Structural characteristics and UV-light enhanced gas sensitivity of La-doped ZnO nanoparticles", Materials Science and Engineering B, Vol. 141, pp. 43-48, 2007.
- [22] C. G. Dighavkar, A. V. Patil, S. J. Patil and R. Y. Borse, "Effect on Ethanol Gas Sensing Performance of Cu Addition to TiO<sub>2</sub> Thick Films", Sensors & Transducers Journal, Vol. 116, pp. 28-37, 2010.
- [23] W. Ang, W. Zhao, P. Liu-Hua, L. Wei-Wei, X. Li, D. Xiao-Chen, H. Wei, "Room-Temperature NH<sub>3</sub> Gas Sensor Based on Hydrothermally Grown ZnO Nanorods", CHIN. PHYS. LETT, Vol. 28, No. 8 , pp. 080702, 2011.
- [24] J.M. Wagh S, G. Jain H, D. Patil R, S. Patil A and L. Patil , A Sensors and Actuators B: Chem, " Modified zinc oxide thick film resistors as NH<sub>3</sub> gas sensor" Vol. 115, pp.128-133, 2006.
- [25] Z. Fan and G. Jia. Lu, "Chemical Sensing with ZnO Nanowires", Department of Chemical Engineering and Materials Science & Department of Electrical Engineering and Computer Science, University of California-Irvine, Irvine, 2005.
- [26] S.T. Shishiyanu, T.S. Shishiyanu, O. I. Lupan, " Sensing characteristics of tin-doped ZnO thin films as NO<sub>2</sub> gas sensor", Sensors and Actuators B , vol. 107, pp. 379–386 2005.
- [27] W. Widanarto, C. Senft, O. Senftleben, W. Hansch, I. Eisele, " Characterization and Sensing Properties of ZnO Film In FG-FET Sensor System for NO<sub>2</sub> Detection" , International Journal of Basic & Applied Sciences, Vol: 11 No: 01, 2011